# Research & Reviews: Journal of Chemistry

# Understanding to Hierarchical Microstructures of Crab (*Chinese Hairy*) Shell as a Natural Architecture

Chuanqiang Zhou[1]*, Xiangxiang Gong[1,2] and Jie Han[2]

[1]Testing Center, Yangzhou University, No. 48 Wenhui East Road, Yangzhou, PR China
[2]School of Chemistry and Chemical Engineering, Yangzhou University, Yangzhou, PR China

## RESEARCH Article

**\*For Correspondence**

Chuanqiang Zhou, Testing Center, Yangzhou University, No. 48 Wenhui East Road, Yangzhou, PR China, Tel: +8651487979383; Fax: +8651487979244

**E-mail:** cqzhou@yzu.edu.cn

### ABSTRACT

This work was done to better understand the microstructures, composition and mechanical properties of *Chinese hairy* crab shell. For fully revealing its hierarchical microstructure, the crab shell was observed with electron microscope under different magnifications from different facets. XRD, EDS, FTIR and TGA techniques have been used to characterize the untreated and chemically-treated crab shells, which provided enough information to determine the species and relative content of components in this biomaterial. Combined the microstructures with constituents analysis, the structural principles of crab shell was detailedly realized from different structural levels beyond former reports. To explore the relationship between structure and function, the mechanical properties of shell have been measured through performing tensile tests. The contributions of organics and minerals in shell to the mechanical properties were also discussed by measuring the tensile strength of de-calcification samples treated with HCl solution.

## INTRODUCTION

Nature always inspires us to develop new technologies or materials through a variety of ways for satisfying the increasing demand occurred in the advancing process of world [1]. Studying biomaterials is an effective strategy for human to obtain accessible wisdom for designing multifunctional man-made materials. Biomaterials have been optimized in structures and compositions in a long selection and evolution process during evolution, and thus possessed exceptional performances (such as mechanical properties) beyond those that can be achieved using synthetic materials with the same components [2,3]. The arthropod exoskeletons, such as lobster cuticle and crab shell, have become one of the most striking biomaterials due to the sophisticated hierarchical organizations. This material was generally deemed to be composed of a thin and waxy layer epicuticle as the waterproofing barrier, and the main structural part (procuticle) designed to resist mechanical loads [4,5]. According to the previous researches [6,7], the procuticle with well-defined micro-architecture were constructed stage by stage according to five structural levels: from fibrils, to fibers, to fiber-based bundles, to planes, and finally to twisted plywood structure. Unfortunately, many details to the microstructures of arthropod cuticle have not been elaborated in these existing reports, which did hinder the further understanding to its conformation. On the other hand, it was reported that the chemical compositions in this biomaterial mainly included long-chain polysaccharide chitins, proteins, and calcite or amorphous calcium carbonate [8-10]. However, there are few investigations involving to the subject how these compositions construct the hierarchical structures of this material so far [11]. To date, the multilevel exoskeleton of arthropod is not fully cognized yet due to its complexity, and thus it is very necessary to study synchronously the structures and chemical compositions for exploring its structural organization.

The multifunctional arthropod exoskeleton not only provides environmental protection and resistance to desiccation, but also supports the bodies, resists mechanical loads [12-14]. The excellent mechanical properties of prawn exoskeleton and crab shell were first found in 1975 by Joffe and Hepburn [15,16]. Melnick et al. reported later the hardness and toughness of crab chela, and pointed out that the dark region in the material showed better mechanical strengths than light-colored one [17]. Recently, Raabe and co-workers explored the influences of microstructure on mechanical properties of lobster cuticle (*Homarus americanus*)

[18-20]. As well known, the mechanical significance of both microstructure and components is vital to manifest structure-property relationships [21,22]. Regrettably, spare researchers could distinguish the contributions of different compositions to the mechanical properties of arthropod exoskeleton.

In this study, the organization conformation and the mechanical properties of the shell of *Chinese hairy* crab are carefully studied through probing microstructures, analyzing chemical composition and performing tensile testing experiments. This study is done to understand the relationship between structural organization and mechanical properties. Another motivation for this research is to reveal the mechanisms how nature creates strong and tough materials by utilizing relatively weak constituents (chitin, protein and carbonates).

# MATERIALS AND METHODS

### Untreated and treated crab shells

Untreated shells of *Chinese hairy* crab were obtained from the local restaurants on the lakefront of Yangcheng Lake located in the city of Suzhou. The wet fresh shells **(Figure 1a)** were peeled manually off from living *Chinese hairy* crab, washed several times with de-ionized water, and then stored in water until the usage. The dry samples were prepared from wet ones by air-drying for 24 h under a relative humidity of ~40%.
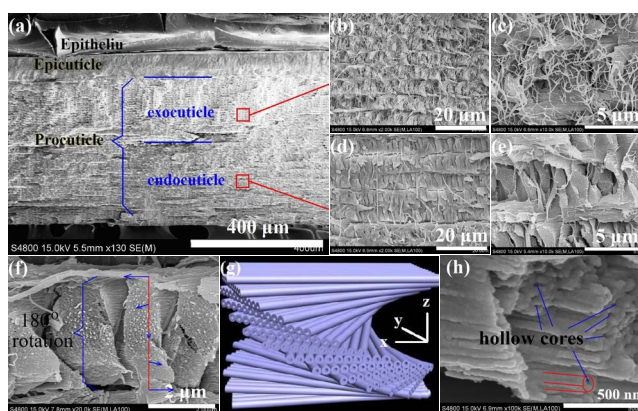


**Figure 1.** (a) FESEM image showing a whole cross-section of crab shell, insert gives a photograph of fresh shell of *Chinese hairy* crab; (b, c) Side-viewed FESEM images of exocuticle; (d, e) Side-viewed FESEM images of endocuticle; (f) Cross section of a plywood layer in endocuticle; (g) A 3D model of a twisted plywood structure; (h) A magnified tips of fiber bundles exhibiting that several parallel-arrayed fibers assemble into a hollow bundle.

For gaining chemically-treated samples, the fresh crab shell fragments were refluxed in 5 wt% NaOH for 6 hours under vigorous stirring to remove most of protein, and/or, treated with 7% HCl solution for a given period at room temperature to remove the mineral salts [23].

### Characterization and testing

Morphology of crab shell was examined by field-emission scanning electron micrograph (FESEM, S-4800, Hitachi Co., Japan) after samples were sputtered with gold electrode, and digital photographs were taken by a FUJIFILM Digital Camera (S2000HD). Qualitative energy dispersive X-ray (EDX) spectra of samples without gold-coated treatment were measured using a Kevex EDX detector (Thermo Co., USA) mounted on the environment scanning electron microscope (ESEM, XL-30, Philips Co., Holland). XRD patterns were recorded on an X-ray diffractometer (XRD, AXS D8 ADVANCE, Brucker, Germany) operated at a voltage of 40 kV and a current of 40 mA with Cu $K\alpha$ radiation with the 2θ range from 10 to 80° in steps of 0.04° with a count time of 1 s each time. The FTIR spectra of samples in KBr pellets were carried out on Cary 670 Spectrum (Varian Co., USA) in the range of 400-4000 cm$^{-1}$. Thermo-gravimetric analysis (TGA, Pyris 1, PerkinElmer Co., USA) were performed with heating range from room temperature to 950°C. The relative humidity in a closed room is controlled by three desiccating machines (Mitsubishi Co., Japan). The 3D simulation models of crab shell's hierarchical structures were drawn by using software 3ds max® 7(Autodesk, Inc.). Stress-strain curves of samples were generated by tensile testing machine (Hualong Instrument Factory, China, WDW-5).

# RESULTS

### Microstructures

Shell of *Chinese hairy* crab is firstly observed with FESEM technique from its cross section, with the representative images displayed in **Figure 1.** As evidently seen from **Figure 1a**, the crab shell with a total thickness of ~550 *μ*m is comprised of epithelium, epicuticle and procuticle from outer to inner. The outermost epithelium regarded as a ~10 *μ*m thin film cracks and curls when examining with electron microscope and under the epithelium the epicuticle of *ca.* 70 *μ*m in thickness is compacted by the close particles **(Figure S1)**. Residual segment defined as procuticle (about 470 *μ*m) becomes the main structural part of crab shell and the major object studied in this work. The procuticle which has well-marked plywood (Bouligand) structures, is further

divided into exocuticle (outer, **Figure 1b and 1c**) and endocuticle (inner, **Figure 1d and 1e**). In the exocuticle, a lot of elongated fibers are discovered from **Figure 1b and 1c**, being a feature distinguished from the endocuticle. Comparing **Figure 1b with 1d**, one can discern that the lamellar height in the exocuticle (6.0 $\mu m$) is slightly smaller than that in the endocuticle (6.6 $\mu m$). Close observation to a plywood structure (**Figure 1f**) indicates apparently that the plane consists of self-twisted fiber-bundles with 1.0-1.5 $\mu m$ in width, where some canals between neighboring bundles penetrate this plywood layer. In every bundle, the ~90 nm fibers are stacked in a helicoids fashion and complete an 180° rotation in the z-direction, forming horizontal planes, as illustrated by a 3D model in **Figure 1g**. Besides, it is interestingly found from **Figure 1h** and **Figure S2** that the fiber in the bundle is actually a cluster of parallel-arrayed fibrils (40 nm in diameter), becoming a tube with a 30 nm hollow core.

Notably, a number of ellipse-type cell pores with dimensions of *ca.* 1 × 0.5 $\mu m$ are disclosed from the top view of procuticle **(Figure 2a)**, whose area ratio to whole shell surface is approximately 0.15. In **Figure 2b**, the cell walls (~1.2 $\mu m$ in width) are found to be fabricated by the arrayed fibers parallel to each other along the long axis of the elliptic pore. Careful detection to an edge of cell pore **(Figure 2c)** documents the under fibers stacked in the normal direction appear a fan-shaped radiation marked by lines, which is further simulated with software 3ds max® **(Figure 2d).** The oblique view given in **Figure 2e** shows synchronously the self-twisted fiber-bundles and the ellipse-type cell pores, where the cell pore seen from top-viewed images displays the pore-canal's morphology observed from the side facet. As exhibited in **Figure 2f**, the canals in the neighboring plywood planes are interlinked and connected inside to form the long one. Moreover, some soft and long ribbon-like structures twist in a helical fashion laid in the long canals, whose ratio to canal is about 0.5.
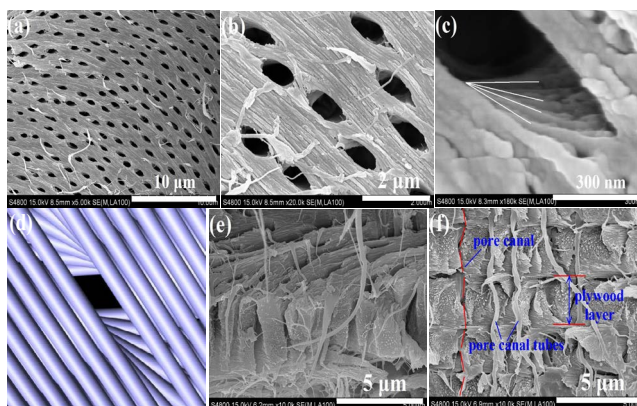


**Figure 2.** (a, b) Top-viewed FESEM images of epicuticle-removed crab shell, showing high-density cell pores in surface; (c) A magnified image to a pore end; (d) A 3D model of a pore canal with twisted plywood structure; (e) An oblique-viewed image for displaying meanwhile the twisted plywood and honeycomb-like pore-canal structures; (f) Side-viewed FESEM image exhibiting a long pore canal, pore canal tubes and plywood layer.

**Figure 3** gives the normalized X-ray diffraction profiles of crab shell powder. In this pattern, three wide diffraction peaks at 19.4, 20.5 and 23.2° are firstly found as the typical feature of crystal α-chitin [23]. A group of diffraction peaks at 2θ=29.6, 36.2, 39.6, 43.4, 47.7, 48.8, 57.8, 61.2, 65.1° can be indexed as the high-crystalline calcite $CaCO_3$, corresponding to 104, 110, 113, 202, 018, 116, 122, 214, 300 planes, respectively (JCPDS Card no. 05–0586). The diffraction signal of (104) plane is much stronger than other ones, indicating that calcite is crystallized along the biopolymer chains. Besides, there are also some obscure and unknown bands found in this pattern, meaning the presence of amorphous components in shell.
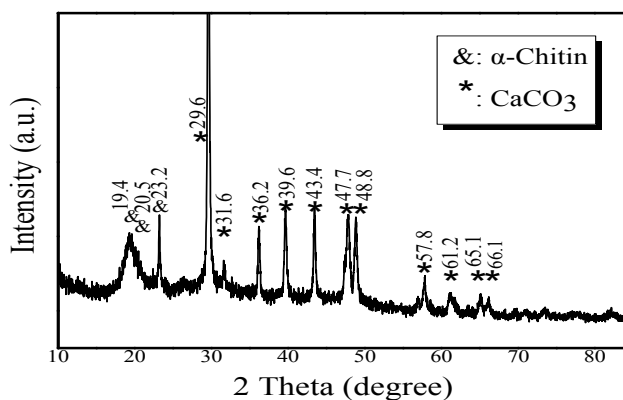


**Figure 3.** XRD pattern of crab shell powder derived from *Chinese hairy* crab.

## Chemically treated materials

Shell of *Chinese hairy* crab is crushed into fragments with approximately 4 × 4 cm in size, and treated with NaOH (for 6 hours) or HCl (24 hours) solution to obtain deproteinated or decalcified sample. Untreated and chemically-treated materials are monitored with EDX, FTIR, TGA and FESEM techniques, respectively. **Figure 4a** gives the EDX spectra of all samples without gold-coated treatment. It is found for untreated shell that the peaks of C, O and Ca elements are very strong, and the signals

of N, Na, Mg, P and Cl signals are relatively weak. As compared to those, the C, N and P peaks of NaOH-treated sample are evidently reduced in intensity, while the HCl-treated shell displays low-level signals of C, O and Ca elements. The sample treated successively by NaOH and HCl solutions only exhibits weakened C and O peaks.
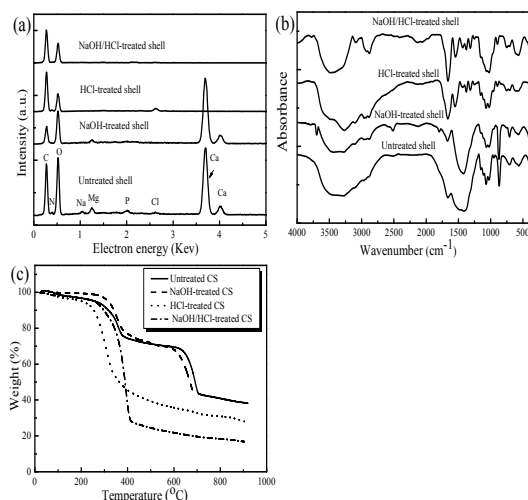


**Figure 4.** EDX analysis (a), FTIR spectra (b) and TGA (c) of untreated, NaOH-treated, HCl-treated and NaOH/HCl-treated crab shells.

FTIR spectra of the untreated and chemically-treated materials are recorded in the range of 400-4000 $cm^{-1}$, and the results are presented in **Figure 4b.** The spectrum of untreated shell is firstly analyzed to estimate its major components: The bands in the range of 3300-3500 $cm^{-1}$ are thought to represent the hydroxyl group, and the characteristic peak at 1662 $cm^{-1}$ indicates amide groups (-NHCO stretching), hinting the presence of protein. The peaks at 711, 870 and 1430 $cm^{-1}$ are attributable to $CO_3^{2-}$ originated from $CaCO_3$ [24]. while the amide II band at 1550 $cm^{-1}$ and NH stretching band at 3272 $cm^{-1}$ [23], are especially characteristic of anhydrous $\alpha$-chitin. The NaOH-treated biomaterials exhibits weak absorbance bands at 3272 (-OH) and 1662 $cm^{-1}$ (-NHCO) due to the removal of protein, while those bands owning to $CO_3$ are reduced even disappear in the spectra of the HCl-treated samples. The NaOH/HCl-treated shell shows only the characteristic bands of chitin in its spectrum.

**Figure 4c** displays thermo-gravimetric analysis (TGA) curves of the untreated and treated samples as the temperature increases from 25 to 900°C. To avoid the interference of water during TGA analysis, all samples are absolutely dried and analyzed under a relative humidity lower than 30%. The first mass reduction found in the curve of untreated sample at about 87°C, cannot be seen in the curve of NaOH-treated (de-proteinated) crab shell, indicative of the decomposing of proteins. Another distinct mass reduction of solid curve is near to 687°C should be due to the decarboxylation of the $CaCO_3$ [19], because this loss does not appear in the curve of HCl-treated sample. Besides, a clear weight drop in the range of 260~550°C is also seen in all curves, which might originate from the degradation of chitin component [25].

The top-view morphologies of untreated and treated shells are presented in **Figure 5.** The untreated bio-material discloses evidently a well-defined porous structures fabricated by the intersected fiber-bundles with smooth surface **(Figure 5a).** In **Figure 5b** and insert, many irregular granules or knobbles are found on the surface of the deproteinated fiber-bundles. Clearly, the shell fragment demineralized with HCl **(Figure 5c)** is mainly composed of the frameless and soft fibers with ~40 nm in diameter, which is thinner than these fibers in untreated sample (~90 nm, **Figure 1h**). As shown in **Figure 5d**, the NaOH/HCl-treated material displays only fused nanofibers with about 20 nm in diameter and hundreds of nanometers in length.
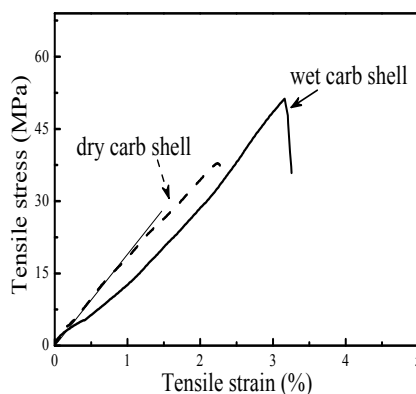


**Figure 5.** FESEM images of untreated (a), NaOH-treated (b), HCl-treated (c) and NaOH/HCl-treated (d) crab shells.

## Mechanics properties

For tensile testing experiment, strip-shaped fragments are cut out from wet and dry crab shells along the head-tail line with

an original length of about 4.0 cm and a width of ~1.0 cm. When testing, one end of shell strip is fixed on the machine and the other is stretched slowly by a stepping motor during measurement. Tensile force and displacement is recorded automatically every 100 ms, and then converted to data of stress and strain, respectively. The typical stress-strain curves of shells in the dry and wet conditions are shown in **Figure 6**, and **Table 1** summarizes the corresponding characteristic mechanical data from the tensile testing.
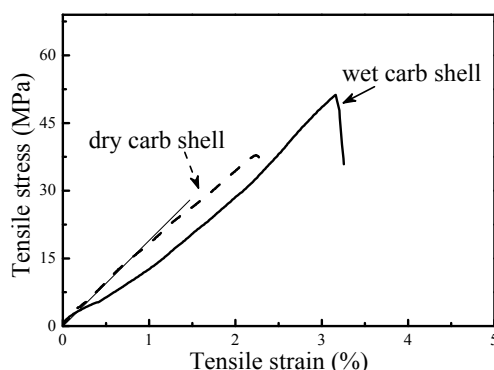


**Figure 6.** Stress-strain curves of the wet and dry shell strip parallel to the head-tail line.

**Table 1.** Mechanical properties of crab shells from tensile testing in the longitudinal direction.

| Sample | E (Mpa) | σf (MPa) | εf (%) | Toughness (Mpa) |
|---|---|---|---|---|
| Hairy crab wet | 1158 ± 85 | 51.2 ± 7.7 | 3.16 ± 0.45 | 0.79 ± 0.18 |
| Hairy crab dry | 1918 ± 132 | 37.8 ± 5.6 | 2.23 ± 0.35 | 0.41 ± 0.09 |
| Mud crab wet (Cameron) | 481 ± 75 | 30.1 ± 5.0 | 6.2 | |
| Mud crab dry (Cameron) | 640 ± 89 | 23.0 ± 3.8 | 3.9 | |
| Sheep crab wet (Chen et al.) | 518 ± 72 | 31.5 ± 5.4 | 6.4 ± 1.0 | 1.02 ± 0.25 |
| Sheep crab dry (Chen et al.) | 764 ± 83 | 12.9 ± 1.7 | 1.8 ± 0.3 | 0.11 ± 0.03 |

The properties are the average including their standard deviation: $E$, Young's modulus; $\sigma f$, stress to fracture; $\varepsilon f$, strain to fracture.

The wet sample has an average ultimate tensile strength of 51.2 ± 7.7 MPa at an average strain to fracture of 3.16 ± 0.45%, while the dry sample breaks at an average ultimate tensile strength of 37.8 ± 5.6 MPa at an average strain to fracture of 2.23 ± 0.35%. The Young's modulus is measured by taking the data points after 1.5% of strain and linear fitting. The average value of Young's modulus for the wet sample is 1158 ± 85 MPa, whereas it is 1918 ± 132 MPa for the dry sample. The work-of-fracture or toughness, as measured by the area under the stress-stain curve, is significantly affected by gradual fracture. The toughness for the wet samples is 0.79 ± 0.18 MPa, which is about two times higher than that for the dry sample (0.41 ± 0.09 MPa).

Tensile testing is also performed to the wet shell strips with the different angle to the head-tail line of crab, and their ultimate tensile strengths and average strains to fracture are shown in **Figure 7a.** When this angle changes from 0 to 22.5, 45, 67.5, 90, 112.5, 135, 157.5° in the shell's plane, the ultimate tensile strengths of crab shells are relatively uniform (~50 MPa), while the average strains of strips fluctuate in the range of 1.8-4.4% when varying the angle. Treating 4 × 1 cm shell strip with HCl solution, the effect of de-mineralized time (DT) on the carbonate content and ultimate tensile strength of such strip are revealed in **Figure 7b.** It is found that the carbonate content of shell seems to descend linearly from 32.02 to 8.64% in the beginning 4.5 hours of treatment. After another 2 hours, the decline of carbonate content in material slows down from 5.85 to 3.53% as the HCl-treated time increases to 12 hours. As for the evolution of the stretch property during de-mineralized process, two evident exhaustion steps are seen in the stress-DT curve. The first strength reduction of the strip takes place at 0~0.5 hour of treatment, rapidly descending from 51.24 to 31.83 MPa. After a flat step, the stress curve undergoes the second exhaustion at 3~4.5 hour of de-mineralized time, reducing from 29.5 to 20.28 MPa in tensile strength. Subsequently, the stress of the shell strip slowly drops and achieves to 18.51 MPa for the treatment of 12 hours with the carbonate content of about 3.53%.

# DISCUSSION

### Structural organization

Morphological observations to the crab shell in this report inform us some new findings on the microstructure of arthropod exoskeletons. The outermost epithelium of shell of *Chinese hairy* crab which should be composed of the organic matrix due to its fragile feature, was seldom mentioned in former researches. The waxy epicuticle is often referred as an external layer and a permeability barrier to the environment [11,19]. Beneath the epicuticle is the procuticle as the main structural part, which is primarily designed to resist mechanical loads [26]. Many elongated fibers are found in exocuticle of crab shell, which is agreement to other report (Guiraud-Guille et al.). Different from the reported arthropod exoskeletons, the thickness difference of plywood in exocuticle and endocuticle for *Chinese hairy* crab shell (~0.5 *μ*m) is much smaller than those (>10 *μ*m) for other crab shell and lobster cuticle [20,22]. Again, the hollow fibril-clusters assembled by nano-fibrils as subordinate structural units, are discovered in this report for the first time. The ribbon-like structures marked in **Figure 2f** are actually pore-canal tubules used to transport nutrients for the growth of crab shell [10,18]. There should be about 1.7 × 10$^{11}$ tubules per m$^2$ for the shell of *Chinese hairy* crab, which is close

to the high density of tubules in other crabs [22,27]. The reason to why only few pore-canal tubules are observed from **Figure 2a,** is that these organic tubes are often destroyed by high-energy electron beam.
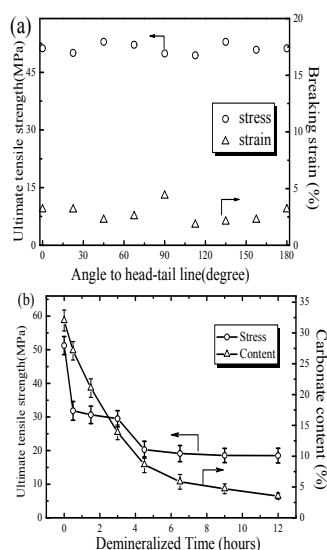


**Figure 7.** (a) Ultimate tensile strengths and breaking strains of the wet shell strips with the different angles to the head-tail line of crab, the insert image marking the directions of these strips from the crab shell; (b) Ultimate tensile strengths and carbonate contents of the wet shell strips with the different de-mineralized treated time in 7% HCl solution.

Interestingly, these side-viewed images of crab shell **(Figure 1)** show the plywood architectures, while the porous structures are observed from the top-viewed photographs of the same shell **(Figure 2).** Although two distinct morphologies could be referred by other researchers, their unity has been not well understood so far due to the complexity of arthropod exoskeletons. Herein, we try to consolidate the plywood and porous structures and delineate the real microstructures of crab shell. It is speculated that the ellipse-type cell pores seen in **Figure 2a** are formed by intersecting of fiber-bundles observed in **Figure 1f**, which is proved by several examples as follow: Firstly, the width of the bundles (1.0-1.5 $\mu m$) is well agreement with that of cell walls (~1.2 $\mu m$). Secondly, the fan-shaped radiation of underlying stacked fibers **(Figure 2c)** hints the rotation of fiber planes below the surface of porous structure. Thirdly, the oblique-viewed image in **Figure 2e** synchronously exhibits plywood layer and porous structure. What is more, a 3D model given in **Figure 2d** predicts a possibility that the cell pores could be indeed constructed by these network-like intersected fiber-bundles.

The chemical constituents of crab shell are revealed by XRD, EDS, FTIR and TGA data. XRD results indicate that the natural crab shell is complex containing at least the crystalline α-chitin and the calcite crystallized along the biopolymer chain. After that, the crab shell pieces are chemically treated by strong basic or acidic solution to remove acidic organics or mineral salts [23]. The sample treated with NaOH solution shows low-level C, N and P elements **(Table S1)**, as well as the weak absorbance bands of hydroxyl group and amide groups **(Figure 4b)**, indicative of the presence of protein in original biomaterial [18,26,28]. The existences of mineral $CaCO_4$ and chitin in the crab shell are again confirmed by the EDS and FTIR results, respectively. In a word, the major components of crab shell should contain protein, carbonates and chitin. Since the thermal degradation temperatures of proteins, chitin and $CaCO_3$ are suggested to be 87°C, 260°C and 687°C by TGA curves, respectively **(Figure 4c)**, their relative contents in this natural biomaterial are tentatively estimated, that is, 5.17% proteins, 24.60% chitin, 32.02% $CaCO_3$, and 38.21% others **(Table 2).**

**Table 2.** The relative contents of major components in raw crab shell measured by TGA techniques.

| Component | Protein | Chitin | CaCO₃ | Others |
|---|---|---|---|---|
| Weight (%) | 5.17 | 24.6 | 32.02 | 38.21 |

To gain insight into the growth principle of arthropod exoskeleton, the structural organizations of shell of the *Chinese hairy crab* are analyzed from the bottom up based on the above-mentioned investigations: At the molecular level, several long-chain polysaccharide chitins are aligned in an anti-parallel manner that gives rise to α-chitin crystals in the form of thinner fibrils with hundreds of nanometers in length [26]. These chitin fibrils are wrapped and bound by proteins and other organics to construct the organics nano-fibers. These strands of organic nano-fibers as matrix are further embedded in the minerals mainly crystalline $CaCO_3$, forming mineral-coated complex fibers (~40 nm) visible in **Figure 1h** [23]. In this example, the coating of minerals onto organic fibers can be evidenced by the fact that the dissolution of biopolymer proteins causes the peeling of some mineral nano-particles from the complex fibers **(Figure 4b)**. And then, these complex fibers array parallel along their axis to form the hollow fiber-clusters displayed in **Figure 1h** and **Figure S2.** Subsequently, these fiber-clusters stack in the normal direction and form lager bundles accompanied with 180° rotating in helicoids fashion **(Figure 1f).** Furthermore, many twisted fiber-bundles as building blocks intersect each other to fabricate the 2D plywood planes widely discovered in the arthropod exoskeletons, showing porous

surface from the top view. Finally, plywood layers referred as Bouligand structures superimpose repeatedly and are adhered with the carbonate salts to generate a multi-layer shell [19,20].

**Mechanics properties**

Mechanical properties of crab shell are exploited to understand the role of structural organization in loads. The concave-shaped stress-stain response seen from **Figure 6** means the plastic deformation for crab shell [18]. Compared with the shells of mud and sheep crab reported previously, the ultimate tensile strengths and Young's modulus of *Chinese hairy* crab are very higher for both wet and dry samples, which may due to the larger contents of inorganic minerals and the interlocked microstructures of the biomaterials [27,29]. However, the *Chinese hairy* crab shell (both wet and dry) has lower values in the average strain to fracture and toughness related to other crab shells, because of the relatively-low content of chitin-protein matrix [22]. Varying the tensile directions in the shell's plane, the ultimate tensile strength does not change too much with the discrepant deformability **(Figure 7a)**, which is interpreted by a fact that the twisted plywood structure of crab cuticle generates the isotropous stretch property [19].

The contribution of minerals in shell to the stretch property is discussed through analyzing the relationships between the tensile strength with the calcium content **(Figure 7b).** The linear decline in calcium content observed in the beginning stage of HCl treatment causes by the dissolving of carbonates which joint the plywood planes with the large cracks **(Figure 2f)** and are exposed in acid solution. In the case, if the stress imposes onto such treated strip, the plywood layers would dislocate because of the deficiency of jointing forces from minerals [30], which thus produces a reduction in tensile strength of shell strip at 0~0.5 hour of treatment **(Figure 7b).** As the minerals between planes are depleted, the inner carbonates coated onto organic fibers begin to be slowly reacted due to the limited diffusion of inorganic acid in porous material [31], thus leading to the delaying release of calcium salts. When the continuity of minerals along the protein-chitin fibers is destroyed by the reaction [21], the contribution of calcium carbonate to tensile strength would be dismissed, corresponding to the second exhaustion in stress curve. Ultimately, the final tensile stress (18.5 MPa) should be mainly attributed to the organic fibers, where the carbonate content of the treated strip is very low (3.53%). Accordingly, the contribution of calcium carbonate to tensile strength is estimated to be 32.7 MPa. This approach for testing the contribution of different components to tensile strength should be very important for materials scientists to realize the design and mechanical properties of natural composites, for developing novel composite materials with enhanced functions.

# CONCLUSION

It is concluded from this works that the shell of *Chinese hairy* crab has the hierarchical structural organization and outstanding mechanical properties. The plywood architectures seen from side-viewed images of crab shell are consolidated with the porous structures observed from the top-viewed photographs for the first time. Chemical analysis to crab shell has indicated that this biology material is comprised of 5.17% proteins, 24.60% crystalline chitin, 32.02% crystalline $CaCO_3$, and 38.21% others. The structural organizations of shell are deduced from the bottom up according to such sequence: crystalline fibrils of chitin, organics/ mineral fibers, hollow fiber-clusters, twisted fiber-bundles, plywood planes, multi-layer shell. Shell of *Chinese hairy* crab possesses excellent Young's modulus and ultimate tensile strength with respect to other crab shell, which seems to be independent of the tensile directions in the shell's plane. The testing to the decalcified samples documents that the contributions of the minerals and the organic fibers in crab shell to tensile strength are 32.7 and 18.5 MPa, respectively, which is the first approach to studying the relationship between mechanical properties and constituents. It should be very important for materials scientists to realize the design and mechanical properties of natural composites, for developing novel composite materials with enhanced functions.

# ACKNOWLEDGEMENTS

# REFERENCES

1. Zhang S. Fabrication of novel biomaterials through molecular self-assembly. Nat Biotechnol 2003; 21: 1171-1178.

2. Burg KJL, et al. Biomaterial developments for bone tissue engineering. Biomaterials 2000; 21: 2347-2359.

3. Puleo DA and Nanci A. Understanding and controlling the bone-implant interface. Biomaterials 1999; 20: 2311-2321.

4. Bouligand Y. Twisted fibrous arrangements in biological materials and cholesteric meso phases. Tissue Cell 1972; 4: 189-217.

5. Giraud-Guille MM. Fine Structure of the chitin-Protein System in the crab cuticle. Tissue Cell 1984; 16: 75-92.

6. Roer R, Dillaman R. The structure and calcification of the crustacean cuticle. Am Zool 1984; 24: 893-909.

7. Giraud-Guille MM, et al. Chitin crystals in arthropod cuticles revealed by diffraction contrast transmission electron microscopy. J Struct Biol 1990; 103: 232-240.

8. Weiner S and Addadi L. Design strategies in mineralized biological materials. J Mater Chem 1997; 7: 689-702.

9.    Lowenstam HA. Minerals formed in organisms. Science 1981; 21: 1126-1131.

10.   Raabe D, et al. Microstructure and crystallographic texture of the chitin-protein network in the biological composite material of the exoskeleton of the lobster *Homarus Americanus*. Mater Sci Eng A 2006; 421: 143-153.

11.   Romano P, et al. The exoskeleton of the lobster *Homarus Americanus* as an example of a smart anisotropic biological material. Acta Biomater 2007; 3: 301-309.

12.   Vincent JFV. Arthropod cuticle: a natural composite shell system. Composite A 2002; 33: 1311-1315.

13.   Vincent JFV and Wegst UGK. Design and mechanical properties of insect cuticle. Arthropod Struct Dev 2004; 33: 187-199.

14.   Sanchez C, et al. Biomimetism and bioinspiration as tools for the design of innovative materials and systems. Nat Mat 2005; 4: 277-288.

15.   Joffe I, et al. Mechanical properties of a crustacean exoskeleton. Comp Biochem Physiol 1975; 50: 545-549.

16.   Hepburn HR, et al. Mechanical properties of a crab shell. Comp Biochem Physiol 1975; 50: 551-554.

17.   Melnick CA, et al. Hardness and toughness of exoskeleton material in the stone crab *Menippe merceharia*. J Mater Res 1996; 11: 2903-2907.

18.   Sachs C, et al. Experimental investigation of the elastic-plastic deformation of mineralized lobster cuticle by digital image correlation. J Struct Biol 2006; 155: 409-425.

19.   Sachs C, et al. Influence of microstructure on deformation anisotropy of mineralized cuticle from the lobster *Homarus americanus*. J Struct Biol 2008; 161: 120-132.

20.   Fabritius H, et al. Influence of structural principles on the mechanics of a biological fiber-based composite material with hierarchical organization: the exoskeleton of the lobster *Homarus americanus*. Adv Mater 2009; 21: 391-400.

21.   Nikolov S, et al. Robustness and optimal use of design principles of arthropod exoskeletons studied by ab initio-based multiscale simulations. J Mech Behav Biomed Mater 2011; 4: 129-145.

22.   Chen PY, et al. Structure and mechanical properties of crab exoskeletons. Acta Biomater 2008; 4: 587-596.

23.   Ifuku S, et al. Preparation of chitin nanofibers with a uniform width as α-chitin from crab shells. Biomacromolecules 2009; 10: 4584-1588.

24.   Zhou GT, et al. Sonochemical synthesis of aragonite-type calcium carbonate with different morphologies. New J Chem 2004; 28: 1027-1031.

25.   Jayakumar R and Tamura H. Synthesis, characterization and thermal properties of chitin-g-poly(epsilon-caprolactone) copolymers by using chitin gel. Inter J Biol Macromol 2008; 43: 32-36.

26.   Giraud-Guille MM. Plywood structures in nature. Curr Opin Solid State Mater Sci 1998; 3: 221-227.

27.   Hegdahl T, et al. The structure and mineralization of the carapace of the crab (Cancer pagurus L)-1. The endocuticle Zool Scr 1977; 6: 89-99.

28.   Shams MI, et al. The transparent crab: preparation and nanostructural implications for bioinspired optically transparent nanocomposites. Soft Matter 2012; 8: 1369-1373.

29.   Cameron JN. Post-molt calcification in the blue crab, Callinectes sapidus-timeing and mechanism. J Exp Biol 1989; 143: 285-304.

30.   Cribb BW, et al. Hardness in arthropod exoskeletons in the absence of transition metals. Acta Biomater 2010; 6: 3152-3156.

31.   Li J, et al. Controlled nanoscale diffusion-limited chemical etching for releasing polystyrene nanocones from recyclable alumina templates. Chem Commun 2012; 48: 11322-11324.